BULLETIN OF THE POLISH ACADEMY OF SCIENCES
TECHNICAL SCIENCES, Vol. 62, No. 3, 2014
DOI: 10.2478/bpasts-2014-0054

Reduction of silicon photomultipliers thermal generation in self-coincidence system applied in low level light measurements

M. BASZCZYK*, P. DOROSZ, S. GŁĄB, W. KUCEWICZ, and Ł. MIK

AGH University of Science and Technology, Department of Electronics, 30 Mickiewicza Ave., 30-059 Kraków, Poland

Abstract. The paper presents method for thermal generation reduction in low level light applications, especially where measured phenomena have random character. The algorithm was developed basing on cosmic ray measurements. The main parts of the system are: Silicon Photomultipliers (SiPM), front-end ASIC for amplifying and shaping signals. SiPM is a very sensitive device which can detect single photons. Comparing to a standard photomultiplier SiPM has a compact size, low operating voltage and it is immune to an electromagnetic field. Thermally generated signals are disadvantage of SiPM. This paper presents the measurement method to reduce influence of thermal generation.

Key words: Silicon Photomultiplier, SiPM, thermal generation, self-coincidence, photon detector, cosmic ray.

1. Introduction

There are many applications based on low level light detection. The most often used sensors are: avalanche photodiodes, standard photomultiplier tubes (PMT), the light-sensitive CCD or CMOS detectors [1-6]. A photomultiplier tube dominates in very small light intensity studies. Among standard silicon detectors an avalanche photodiode has a smaller gain than SiPM [7]. CCD and CMOS sensors have smaller sensitivity than SiPM [8].

The paper describes the measurement system based on SiPM, the used method and results. The construction of SiPM is presented, its advantages and disadvantages with respect to PMT. Principles of work of the front-end ASIC for SiPM are explained.

The cosmic ray phenomenon was used to prove that the presented method for reduction of SiPM thermal generation operates properly. Cosmic rays are particles that are observed to strike the Earth's atmosphere with high energies. It is formed of radiation that is constantly raining down from a space. Showers of high energy particles occur when energetic cosmic rays strike the top of the Earth's atmosphere. An occurrence of cosmic rays has a random character. The cosmic ray could be observed using a scintillator, which converts deposited energy of a passing particle to visible light photons. Such photons are registered by SiPM.

2. Silicon photomultiplier

SiPM is a device which can detect a single photon [7, 9]. SiPM is an array of photodiodes (cells) connected together in parallel (Fig. 1). Each element of this array consists of a diode and a quenching resistor to limit current flowing through the junction.

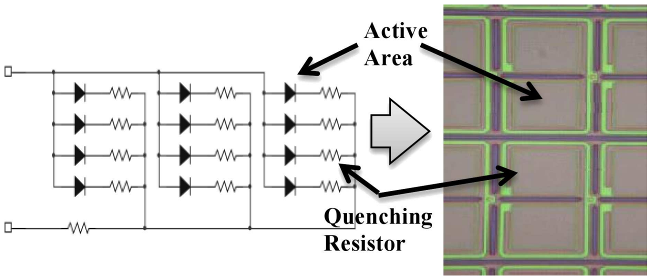

Fig. 1. Silicon photomultiplier construction – electrical schematic and picture of surface under microscope Refs. [10, 11]

The current – voltage characteristic is presented in Fig. 2. At some specific voltage there occurs in a p-n junction the breakdown phenomenon. When SiPM is biased beyond the electrical breakdown voltage – it is operating in the Geiger mode – each generated pair of electron-hole creates an avalanche. A typical gain is between 10^5 and 10^6 electrons per photon [12].

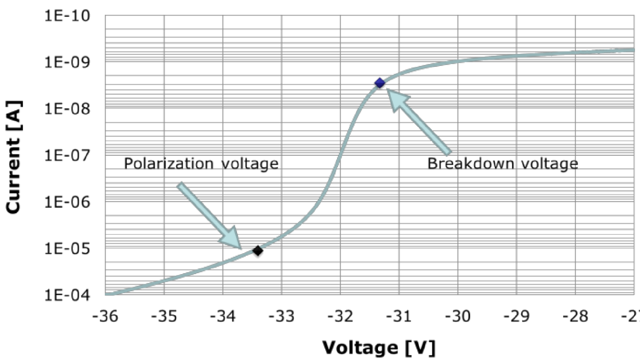

Fig. 2. Current – voltage characteristic of Hamamatsu S10362 measured with semiconductor device parameter analyzer

*e-mail: baszczyk@agh.edu.pl

An isolating ring around a cell prevents an avalanche from spreading outside the cell. The total output is a sum of current from all cells hence it is proportional to the number of avalanches, which in turn is proportional to the light intensity.

The main advantages of SiPM with respect to the standard PMT are: the compact size, low power consumption, low operating voltage and immunity to electromagnetic field. Operating voltage of SiPM depends on the detector's type and is lower than 100 V.

The main disadvantage of SiPM is dark current caused by thermally generated avalanches. In this phenomenon avalanches could be generated even if a photon was not detected. Electrical signals from thermal generation are the same like those from photons. Dark Count Rate (DCR) defines how often thermally generated avalanches appear [13].

The Hamamatsu's S10362-11-50U Silicon Photomultiplier has been used in an experiment. Parameters of this detector are presented in Table 1.

Table 1
Parameters of Hamamatsu SiPM after Ref. [11]

Parameter	S10362-11-50U	Unit
Effective active area	1	mm^2
Number of pixels	400	–
Pixel Size	50×50	μm
Photon Detection Efficiency	50	%
DCR	400	kcps (kilo counts per second)

3. Front-end ASIC

The front-end ASIC was developed to amplify and shape signals from Silicon Photomultiplier. The designed integrated circuit consists of three crucial elements: preamplifiers, pole-zero cancellation circuit (PZC) and peak detector and hold circuit (PDH).

The current signal from SiPM rises very quickly but falls rather slowly. In order to perform next measurement, the previous avalanche has to be completely discharged. To keep measuring at a proper rate a falling edge of SiPM's signal has to be as short as possible. PZC fulfills these requirements and normalizes the signal in time to avoid undershoots and overshoots of signals.

The ASIC consists of four channels. Each channel is able to perform measurements in parallel. A signal from SiPM can be measured in two ranges of gain: high and low.

The amplitude on the preamplifier's output is proportional to the number of avalanches appearing in SiPM, it is necessary to detect the peak amplitude and hold it for an analog to a digital conversion in ADC. This is done by a peak detector and a hold circuit.

The ASIC has two independent comparators for each channel and enables to change the comparator's threshold separately in each one. More precise information about the front-end ASIC are in [14].

Figure 3 shows signals of the amplifier's output of ASIC in a persistence mode. This mode allows to observe signals for chosen time interval and present them together on a single plot. It shows some specific levels of amplitude. Each level represents different number of photons registered by a detector in a single measurement. The first level corresponds to one photon, second level corresponds to two photons, etc.

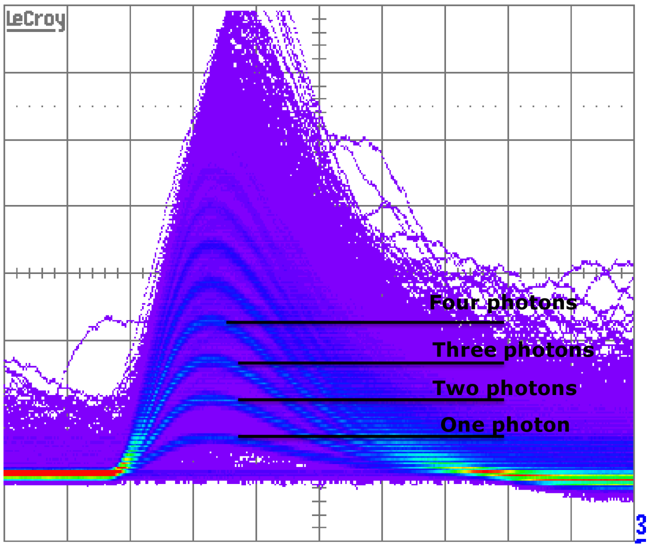

Fig. 3. Signals from SiPM in time domain with persistence mode

4. Optical block with scintillator

Scintillators are materials which rely on the emission of photons from the excited states. They are widely used to measure radiation. In the presented measurement system a scintillator converts cosmic rays to light which is detected by SiPM [15]. The wavelength shift fiber (WLS) is the connection between scintillator and SiPM. The fiber is made from a scintillator material – Kurraray's plastic scintillator fiber. Maximum of absorption spectrum for the WLS is equal to 430 nm. For emission this spectrum is shifted towards 480 nm [16, 17].

Figure 4 shows an optical block set up. In the center of a scintillator there is a groove where a fiber was placed. To provide the best connection between these two parts optical grease was used. Optical grease has a similar refractive coefficient to that of the WLS fiber. As a result, the reflection is reduced and more photons generated in scintillator can enter the fiber.

Fig. 4. WLS fiber placed in scintillator's groove

At the ends of WLS fiber there are SMA adapters. To couple SiPM and WLS fiber a special connector was made (Fig. 5). It enables to make a replaceable block for a detector and place the fiber's end on the center of an active area of the detector. This connection is crucial for the level of efficiency.

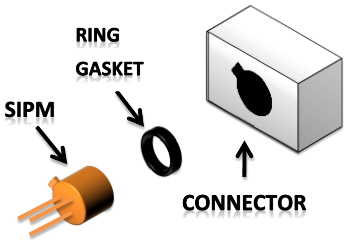

Fig. 5. Schematic block for SiPM and SMA connector

Every part of the measurement system must be placed in a dark box (Fig. 6). It helps in minimizing the impact of the outside light and increases accuracy in measurements of the dark count rate and cosmic ray.

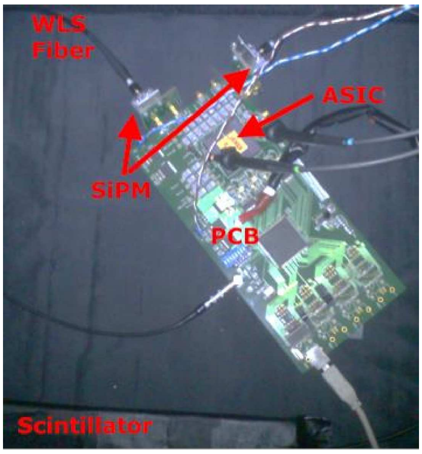

Fig. 6. Measurement system in dark box

5. Data Acquisition System

The schematic of data acquisition system is presented in Fig. 7. Optical signals are going from scintillator to SiPMs. Detector converts optical signal to electrical form. Electrical signal flows through two channels of ASIC in parallel. FPGA controls the data flow in the system. It gathers data from analog to digital converters, gets information from comparators, provides information about time and sets needed parameters of ASIC.

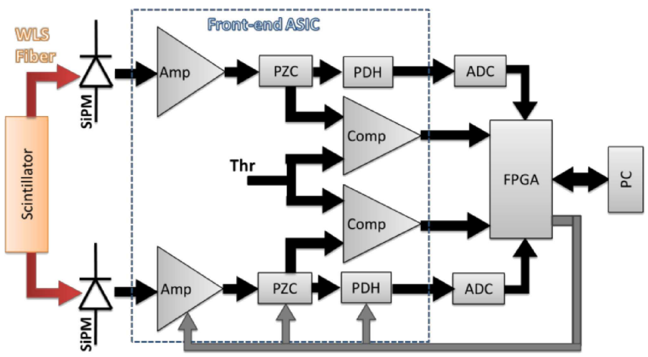

Fig. 7. Data acquisition system with scintillator, WLS fibers, SiPM, Front-end ASIC, ADC, FPGA

The coincidence system is a crucial element in the data acquisition system. It was implemented in FPGA. The SiPM generates signals from detected photons and also generate thermal signals. Coincidence enables to distinguish these signals and can reduce influence of thermal generation on the measurement. In effect data which are probably produced by cosmic ray are gathered.

The coincidence block gives an opportunity to set two modes of operation (Fig. 8). First mode provides simple logic conjunction. If signals from both comparators are active a coincidence signal is also active and the data are collected.

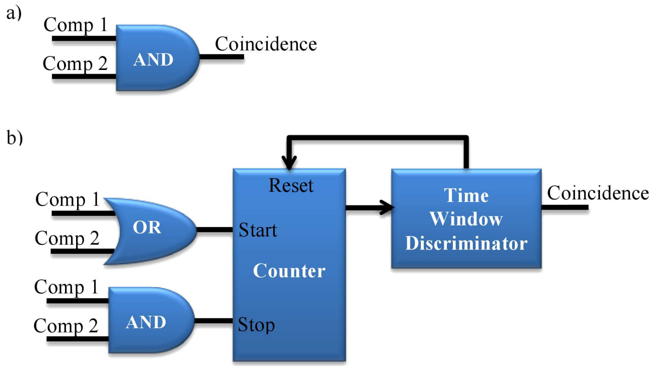

Fig. 8. Coincidence block a) in logic conjunction mode b) in time window mode

Second mode enables to set a time window. When a signal from one comparator is active a system waits for a fixed time. If during this fixed time second comparator becomes active then coincidence occurs, if not a system ignores coming data. The time window discriminator block will reset counter. The time of the coincidence window can be changed.

PC application provides graphical interface to control the system and gather data. Data can be collected in two ways: as histogram to speed up the measurement or every single record to receive more precise information. The second method provides information about amplitudes from two channels and time between following events.

6. Results

6.1. Thermal generation. Measurements of thermal generation were carried out. An oscilloscope was used to observe data and signals from coincidence. Figure 9 shows oscilloscope waveforms. Coincidence signals were connected as a trigger input. Signals from ASIC's amplifiers from both channels were connected to the oscilloscope. Waveforms were gathered with the same persistence as setting up the time option and in the same temperature. On the top of each subfigure a coincidence signal is presented. Lower there are signals from two channels. The comparator threshold was set at the level of 2.5 photoelectrons.

Figure 9 shows main differences between the two presented modes. In the time window mode the coincidence time is fixed and is equal to 12 ns. Time of coincidence in a conjunction mode changes up to about 100 ns. Voltage pulses at amplifier outputs have the duration of 100 ns, therefore comparators also last 100 ns. It leads to situations, where a coincidence signal is generated even when pulses on both channels appear with the 100 ns delay. When there is no delay between channels it can be seen that coincidence lasts as long as a comparator signal (100 ns). This two extreme situations, are presented in Fig. 10. It is the reason why an oscilloscope gathered more events in the logic conjunction mode (2043 sweeps) than in 12ns time window mode (437 sweeps).

a) logic conjunction mode

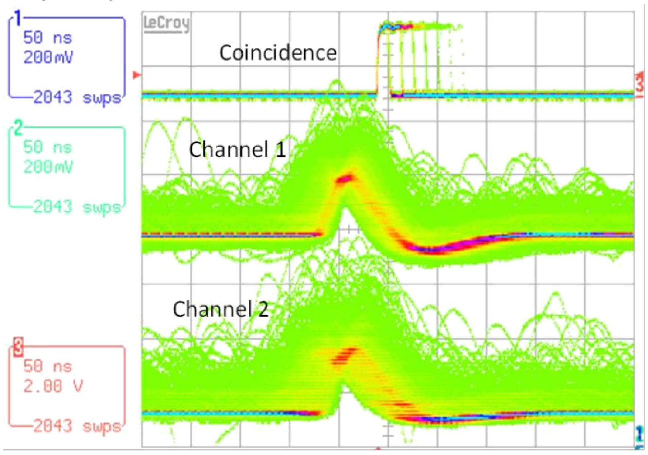

b) 12 ns time window mode

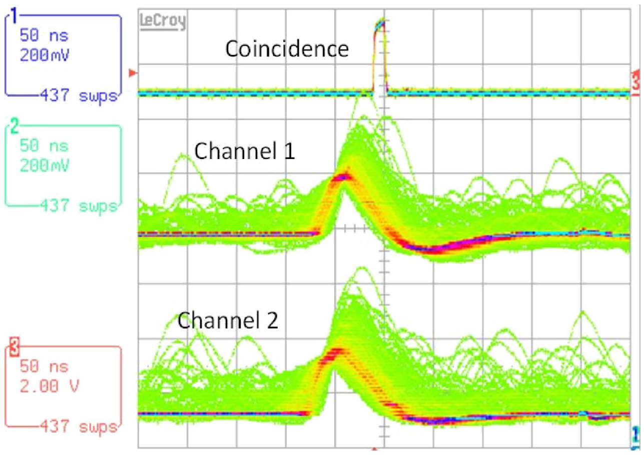

Fig. 9. Thermal generation gathered with the same persistence time and temperature with two coincidence modes

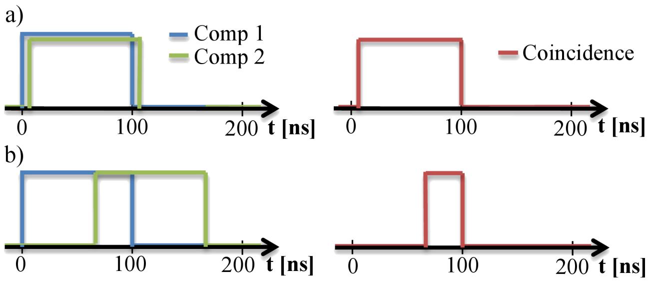

Fig. 10. Coincidence logic conjunction mode a) without delay between comparators, b) with delay between comparators

In the coincidence time window mode dependencies between thermal generation counts and a time window are presented in Fig. 11. Data was gathered using the measurement system and PC application. The bigger coincidence window the higher value of dark count rate appear.

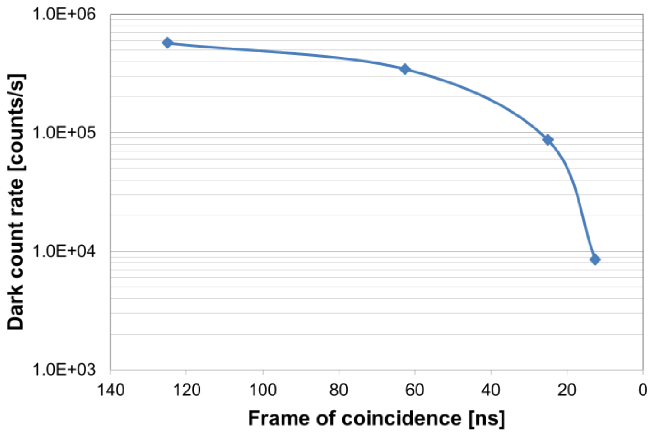

Fig. 11. Dark count rate for different coincidence time windows

The process of thermally generated avalanches is stochastic. Number of those avalanches can be reduced by simultaneous measurements of signals in two or more SiPMs with coincidence [11, 18–20].

The dark count rate of examined SiPM has been on the level of 800 kcps (Table 1). When a measurement system operates in the time window mode and a coincidence signal lasts 12 ns, then the measured dark count rate has the value of 8 kcps. The thermal generation influence was reduced by two orders of magnitude.

6.2. Calibration. An acquisition system has been calibrated before measurements of cosmic rays. It is needed to find dependence between amplitude of frond-end ASIC in ADC unit and number of photons. Calibration was made using the blue LED diode as a light source. The histogram of the signals gathered using the LED diode is presented in Fig. 12. Each peak on histogram corresponds to a different number of photons appearing at the moment of measurement on the surface of SiPM. The first peak refers to one photon, second peak to two photons and so on. Data was gathered in a synchronous way with LED diode pulses. Hence in measurement there is a small number of thermally generated signals.

The Levenberg-Marquardt method was used to find local maxima of the histogram. It minimizes the weighted mean square error between the raw data and the best nonlinear fit f:

$$y[i] = f(x[i], a_1, m_1, \sigma_1, a_2, m_2, \sigma_2 ...).$$

The nonlinear fit curve model f is the sum of Gaussians:

$$f(x, a_1, m_1, \sigma_1, ...) = a_1 e^{\frac{(x-m_1)^2}{\sigma_1}} + a_2 e^{\frac{(x-m_2)^2}{\sigma_2}} + ...$$

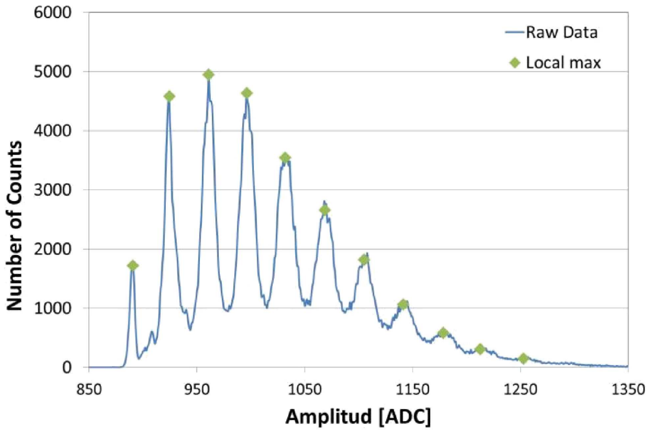

Fig. 12. Histogram of signals gathered synchronous with blue LED

The best fit parameters determined from the Levenberg-Marquardt method are the y and x coordinate of local maxima.

Local maxima were used to calibrate the output signal as a function of a photon number (Fig. 13). From this plot the gain of the detector (amplitude in ADC referring to one photon) can be found. It is equal to 40.6 ADC per photon.

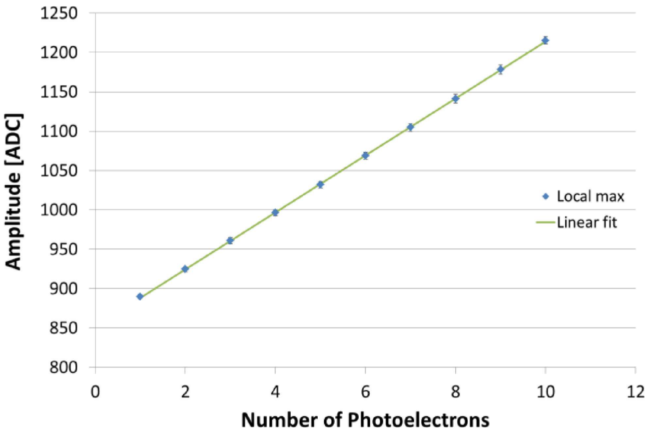

Fig. 13. Linear fit to local maxima of histogram from Fig. 12

6.3. Cosmic ray. The method for thermal generation reduction in low level light applications using a coincidence system with a time window was verified in cosmic ray measurements. This phenomenon has a random character. The cosmic rays measurements are presented in Fig. 14 in a form of histogram. It represents relationship between number of counts for each number of photoelectrons. During measurement the threshold of comparators was set to 2.5 photoelectrons. It can be seen that the thermal generation disturbs measurements in a logic conjunction coincidence mode. Figure 14a has his maximal value just after the threshold. Most of these coincidence events is generated by thermal generation. For the 12 ns time window coincidence mode the maximum value is equal to 12 photoelectron (Fig. 14b). The shape of Fig. 14b corresponds to the Landau shape which is consistent with theory [21].

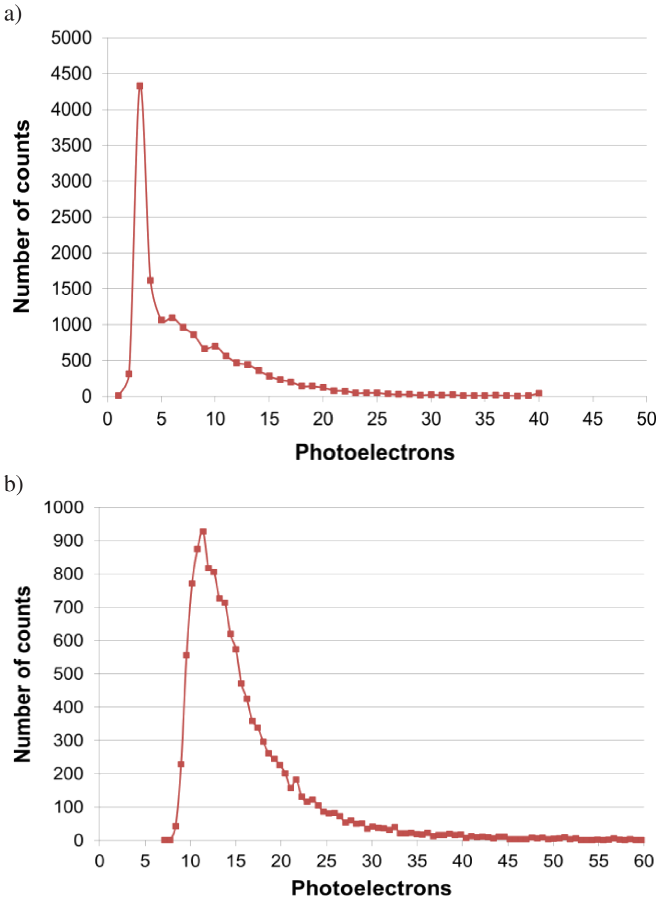

Fig. 14. Cosmic ray measurement, a) coincidence logic conjunction mode, b) coincidence 12ns time window

Figure 15 represents a histogram of time between consecutive events. Influence of thermal generation can be seen here as well. Histogram counts for low time bins in the coincidence logic conjunction mode have higher values.

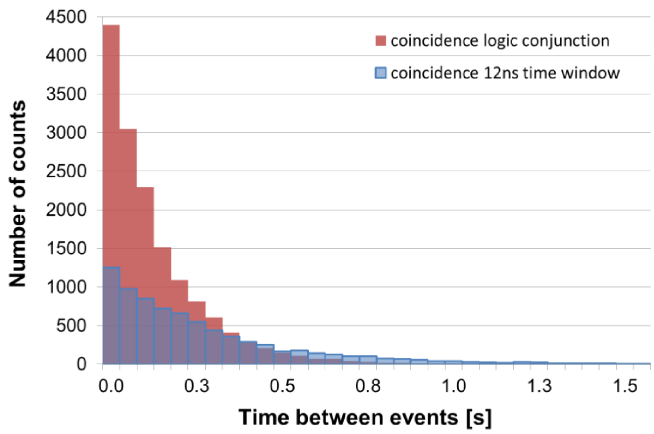

Fig. 15. Histogram of time between consecutive events

7. Conclusions

The method for thermal generation reduction in low level light applications was developed. The measurement system includes silicon photomultipliers with the dedicated front-end ASIC and FPGA driver for single photon detection.

Cosmic ray was used as a signal source of a random character to test self-coincidence performance. The scintillator based optical block was built to measure cosmic ray.

Two coincidence methods were compared: logic conjunction mode and time window mode. In the random signal measurement time window a coincidence mode is more effective. Using this method the dark count rate can be successfully reduced.

Acknowledgements. This work has been partially supported by the statutory activity (11.11.230.017) and faculty grant. The authors thank Istituto Nazionale di Fisica Nucleare Sezione di Ferrara for optical elements required to build the measurement setup.

REFERENCES

[1] A. Roda, M. Guardigli, E. Michelini, and M. Mirasoli, "Bioluminescence in analytical chemistry and in vivo imaging", *TrAC Trends in Analytical Chemistry* 28 (3), 307–322 (2009).

[2] I.F. Castro, A.J. Soares, and J.F. Veloso, "Impact of dark counts in low-light level silicon photomultiplier multi-readout applications", *IEEE Nuclear Science Sym. Conf. Record (NSS/MIC)* 1, 1592–1596 (2009).

[3] M.K. Sasaki, S. Vicente, V. Grassi, and E Zagatto, "Differential Reaction-Rate Methods in Flow Analysis", *Open Analytical Chemistry J.* 6, 28–38 (2012).

[4] Ł. Mik, W. Kucewicz, R. Szczypiński, D.G. Pijanowska, P. Dorosz, M. Baszczyk, S. Głąb, and M. Sapor, "Detection of Fluorescence Light using Silicon Photomultipliers", *Best of East for Eastern Partnership* 1, http://www. bestofeast.mwci.eu. (2011).

[5] R.R. Singh, L. Leng, A. Guenther, and R. Genov, "A CMOS-Microfluidic Chemiluminescence Contact Imaging Microsystem", *IEEE J. Solid-State Circuits* 47 (11), 2822–2833 (2012).

[6] A. Górecka-Drzazga, B.J. Cichy, P. Szczepańska, R. Walczak, and J.A. Dziuban, "Field-emission light sources for lab-on-a-chip microdevices", *Bull. Pol. Ac.: Tech.* 60 (1), 13–18 (2012).

[7] V. Golovin, "Novel type of avalanche photodetector with Geiger mode operation", *Nuclear Instruments and Methods Section* A 518, 560–564 (2004).

[8] "ImageEM – EMCCD technical note", http://www.hamamatsu.com, (2013).

[9] N. Dinu, R. Battiston, M. Boscardin, G. Collazuol, F. Corsi, G.F. Dalla Betta, A. Del Guerra, G. Llosá, M. Ionica, G. Levi, S. Marcatili, C. Marzocca, C. Piemonte, G. Pignatel, A. Pozza, L. Quadrani, C. Sbarra, and N. Zorzi, "Development of the first prototype of Silicon PhotoMultiplier (SiPM) at ITC-irst", *Nuclear Instruments and Methods Section* A 572, 422–426 (2006).

[10] K. Yamamoto, K. Yamamura, K. Sato, T. Ota, H. Suzuki, and S. Ohsuka, "Development of Multi-Pixel Photon Counter (MPPC)", *IEEE Nuclear Science Symp. Conf. Record* 2, 1094–1097 (2006).

[11] Hamamatsu, "MPPC/Technical information", http://www.hamamatsu.com/resources/pdf/ssd/mppc_techinfo_e.pdf (2013).

[12] M. Teshima, B. Dolgoshein, R. Mirzoyan, J. Nincovic, and E. Popova, "SiPM development for Astroparticle Physics application", *Proc. 30th Int. Cosmic Ray Conf.* 5, 985–988 (2007).

[13] M. Ramilli, "Characterization of SiPM: temperature dependencies", *IEEE Nuclear Science Symp. Conf. Record* 1, 2467–2470 (2008).

[14] M. Baszczyk, P. Dorosz, S. Głąb, W. Kucewicz, and M. Sapor, "Four channels data acquisition system for silicon photomultipliers", *Electronics – Constructions, Technologies, Applications* 52 (12), 28–31 (2011).

[15] W. Baldini, M. Benettoni, R. Calabrese, V. Carassiti, G. Cibinetto, F. Dal Corso, F. Evangelisti, C. Fanin, E. Feltresi, N. Gagliardi, E. Luppi, R. Malaguti, M. Manzali, M. Melchiorri, M. Munerato, M. Posocco, A.C. Ramusino, M. Rotondo, R. Stroili, and L. Tomassetti, "A scintillator based muon system with SiPM readout for the SuperB detector", *IEEE Nuclear Science Symp. Conf. Record (NSS/MIC)* 1, 1718–1721 (2010).

[16] *Plastic Scintillating Fibers (Materials and Structures)*, http://kuraraypsf.jp/psf/ (2013).

[17] D. Dorosz, J. Dorosz, A. Zając, J. Żmojda, and M. Kochanowicz, "Active optical fibres for application in laser and broadband ASE sources", *Bull. Pol. Ac.: Tech.* 60 (4), 673–682 (2012).

[18] R. Pagano, D. Corso, S. Lombardo, G. Valvo, C.N. Sanfilippo, G. Fallica, and S. Libertino, "Dark current in silicon photomultiplier pixels: data and model", *IEEE Trans. on Electron Devices* 59 (9), 2410–2416, (2012).

[19] S. Woo-Suk, L. Chae-Hun, and C. Gyu-Seong, "Influence of guard-ring structure on the dark count rates of silicon photomultipliers", *Electron Device Letters* 34 (3), 336–338 (2013).

[20] O. Soto, R. Rojas, S. Kuleshov, H. Hakobyan, A. Toro, W.K. Brooks, and M. Olivares, "Characterization of Multi Pixel Photon Counter (MPPC) array. Statistical approach", *Instrumentation and Measurement Technology Conf. (I2MTC)* 1, 157–161, (2013).

[21] M.S. Longair, *High Energy Astrophysics*, pp. 270–286, Cambridge University Press, Cambridge, 1992.